JOURNAL OF MATERIALS SCIENCE: MATERIALS IN MEDICINE 12 (2001) 327–332

Technique for estimating fracture resistance of cultured neocartilage

MICHELLE OYEN-TIESMA, ROBERT F. COOK
Department of Chemical Engineering and Materials Science, University of Minnesota, Minneapolis, MN 55455, USA

Tensile tests on an artificial tissue of cultured neocartilage are described with a view to obtaining objective criteria for the onset of fracture and to estimating the tissue fracture resistance. The energy dissipation and compliance of the hyperelastic, hysteretic load-displacement responses exhibit great sensitivity to crack propagation during loading. A simple scheme is presented for deconvoluting the energy dissipated by cracking from an overall hysteresis loop and thus estimating the fracture resistance. The results suggest that the apparent fracture resistance of cultured neocartilage is determined by events localized to the crack and may exhibit a transient increase on initial crack extension.

1. Introduction

Articular cartilage is the resilient material covering the ends of long bones, forming the articulating surfaces in diarthrodial joints (*e.g.* knees, elbows, knuckles). In performing its damping and load-distributing function, cartilage is strong in compression, even though it contains only about 30% solids – predominantly type II collagen fibrils and aggrecan proteoglycan aggregates – and 70% water [1]. Both the composition and microstructure of the collagen-proteoglycan matrix of cartilage contribute to its nonlinear viscoelastic mechanical behavior [2]. Although the proteoglycans are very important in the compressive response of cartilage, the collagen network is presumed to be almost entirely responsible for the ''linear-region'' tensile stiffness. The tensile modulus in the linear region of the stress–strain response and the tensile strength are both greatest in the superficial layer of cartilage and decrease with depth [3]. Tensile strength and stiffness both decrease with age in load-bearing tissues [4], and stiffness has also been shown to decrease rapidly during osteoarthritis-like degeneration [5].

The failure of articular cartilage to perform its function – either by change in properties or by removal – results in the disease osteoarthritis, a disabling condition for which there is no available treatment or cure. Fatigue is believed to contribute to the development of primary (old-age) arthritis [6] by gradually fracturing and fibrillating the collagen–proteoglycan matrix. In addition, although arthritis is usually considered a disease of the aged, younger people can be affected when a joint is injured [7, 8]; impact loading can result in cartilage crack formation in addition to bony fracture. Although considerable work has been directed at understanding the viscoelastic behavior of cartilage under physiologic loading conditions, there has been only limited recent recognition of the clinical importance of cartilage fracture mechanics [9].

Our laboratory has developed a method for culturing chondrocytes (cartilage cells) *in vitro* to form an artificial tissue layer suitable for mechanical testing [10]. The ''neocartilage'' is similar in composition to natural cartilage, but lacks a highly organized microstructure: while natural cartilage has distinct layers (zones) and a complicated collagen fibril arrangement, the neocartilage is uniform with a random fibril distribution. Although neocartilage and articular cartilage are not microstructurally identical, the neocartilage culture system allows direct study of the effect of biochemical composition on mechanical properties. Both cyclic tensile tests and a modified single-edge-notch fracture test have been performed on the cultured tissue [10], although a thorough characterization of its mechanical behavior has not been performed.

In this investigation, the energetics of fracture in cultured neocartilage was specifically considered. A primary goal was to develop objective criteria for the determination of when, and if, fracture occurs in the material. (Ideally these criteria would not depend on direct inspection of a specimen.) A secondary goal was the estimation of the energy dissipated during fracture and verification that the fracture energy was separate from the energy losses associated with irreversible viscoelastic or plastic processes. The fracture-energy values along with measured incremental crack length changes allowed fracture resistance to be calculated.

2. Experimental method

Cultured neocartilage was prepared as described previously [10]. Briefly, articular cartilage was harvested from stifle and shoulder joints of young New Zealand White rabbits, following a protocol approved by the Instutional Animal Care and Use Committee (IACUC) at the University of Minnesota. Chondrocytes were isolated by sequential digestion in trypsin and collagenase. The

cells were plated at 2 million cells per 25 cm^2 growth area in flasks coated with denatured type I collagen and cultured for 8 weeks in F12 media with 15% FBS, 0.2% gentamycin, and 30 μg/ml ascorbate.

Tissue from 2 different flasks, 4 samples per flask, was mechanically tested in this investigation. Samples were harvested fresh from culture and tested the day of harvest. Strips approximately 5–6 mm wide by 20–25 mm long were prepared from the 67 μm thick tissue layer. Testing was performed in a mechanical testing machine with specimens submersed in a room-temperature saline bath. The gage length of the gripped samples was approximately 12 mm.

Cyclic tension tests were performed in displacement-control for both unnotched and notched samples. Specimens were cycled 4 times to a peak displacement level and returned to zero displacement at 0.1 mm s^{-1}. Peak displacement levels were 0.8 and 1.1 mm for the tension tests, and 0.8, 1.1, 1.4, 1.7, 2.1, and 2.4 mm for the notched fracture tests, corresponding to approximately 6% and 20% minimum and maximum strain levels, respectively. A fracture test ended when the specimen exhibited complete failure. Each specimen was tested sequentially in tension and fracture, without removing the specimen from the grips. Samples were allowed to ''rest'' for a period of several minutes following the tensile test prior to the fracture test. During this time a notch about 1/3 the width of the sample was cut in the specimen with a sharp scalpel. Load and grip-to-grip displacement data were collected for each test at a sampling rate of 10 Hz.

A high resolution video camera was used to videotape each experiment. Measurements of the initial notch length and the crack propagation in each cycle were made from the video tape at 60 μm resolution. All crack length measurements were made in duplicate.

3. Results and analysis

3.1. Load-displacement measurements

The mechanical behavior of cultured neocartilage was grossly hyperelastic and hysteretic. Fig. 1 shows a typical load-displacement P–u response for an unnotched, notched, and cracking specimen subjected to cyclic tensile displacements. On initial loading, the unnotched specimen exhibited a greater than linear dependence of load on displacement, approximately described by a quadratic, $P \propto u^2$. On unloading, there was distinct hysteresis. Increasing the peak displacement increased the peak load with no other change in behavior. Introduction of a notch into the sample caused an increase in specimen compliance with continued load-displacement hysteresis, and increasing the imposed peak displacement level increased the peak load similarly to that observed for the unnotched specimen. No further changes in material behavior were apparent until a crack began to propagate at the notch root, at which point the load dropped off sharply during increasing displacement and the hysteresis loop opened substantially. This behavior continued until total specimen failure. An example of this sequence is shown in Fig. 2; videotaped frames from the experiment

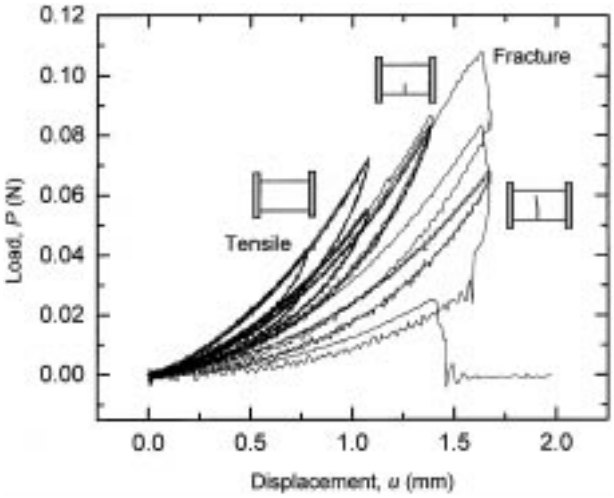

Figure 1 Plot of load, P, versus displacement, u, for a cultured neocartilage specimen tested in tension. Inset schematics indicate the specimen sequentially unnotched, notched, and actively cracking during the test, giving rise to different load-displacement responses.

are shown for the unnotched, notched and cracked specimen at complete unload.

3.2. Dissipated energy

Each load-displacement response for both the tensile and fracture tests was broken down cycle by cycle into a series of loops, consisting of one loading and subsequent unloading cycle (Fig. 3). There were thus 4 cycles for each displacement level in each test; a total of 8 cycles for each tensile test and > 8 for each fracture test. Cycles were numbered sequentially from $n = 1$ to > 16. The total energy in each cycle, $U_T(n)$, was defined as the area between the loading curve and the displacement axis. The dissipated energy in each cycle, $U_D(n)$, was calculated as the area between the loading and unloading curves (Fig. 3a). Calculations of area (energy) were made using trapezoidal integration. For each cycle the ratio of dissipated to total energy $D(n)$ was calculated by

$$D(n) = U_D(n)/U_T(n) \tag{1}$$

and recorded as a function of cycle number (n).

Figs 4(a) and 5(a) show the cyclic P–u responses for notched and fracturing specimens. The open symbols in Figs 4(b) and 5(b) show the dissipated energy ratio $D(n)$ calculated from the load-displacement cycles of Figs 4(a) and 5(a) using Equation (1). For the specimen in Fig. 4(a) no cracking was observed for $n = 1$–12 and $D(n)$ exhibited a slightly decreasing trend with n about $D(n) \sim 0.25$–0.2. On cycles 13 and 14 crack propagation was observed at the notch root and was (subsequently) associated with a significant increase in $D(n)$ to ~ 0.4. On cycle 15, no crack propagation was observed, and $D(n)$ decreased to ~ 0.2; on cycle 16, the crack propagated again with an associated large increase in $D(n)$ and finally on cycle 17, the crack completely fractured the specimen leading to maximum dissipation of $D = 1$. Similar behavior was observed for the specimen in Fig. 5(a); no observed crack propagation

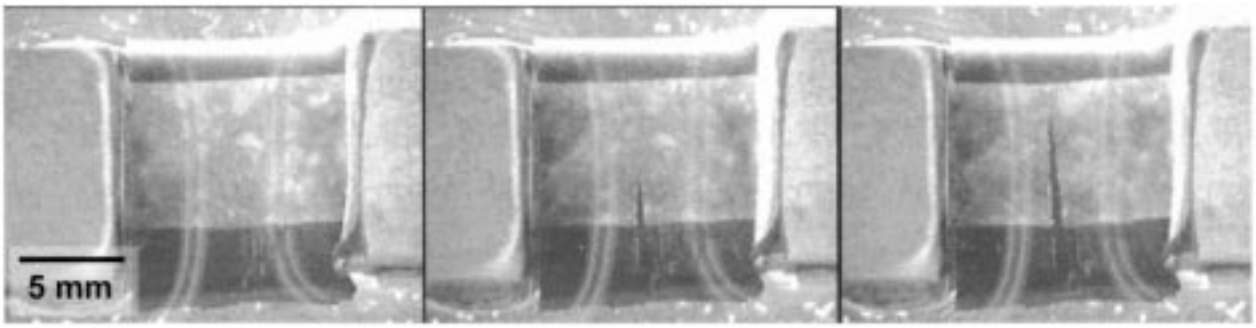

Figure 2 Optical images captured as single frames videotaped from a neocartilage sample during tensile and fracture tests. From left to right, the sample is shown in the unnotched state prior to tensile testing, the notched state prior to fracture testing, and in the cracked state during fracture testing (all zero load).

for $n \leq 12$ followed by crack propagation and increased $D(n)$ on subsequent cycles. In this case, there were two ''arrest'' events characterized by small or negligible crack extension during the cycle and associated decreases in $D(n)$ towards the uncracked level at $n = 16$ and 20, before complete failure at $n = 21$.

Also shown in Figs 4(b) and 5(b) as the solid symbols are the dissipated energy ratios calculated from the *P–u* responses of the (unnotched) tensile specimens. The insensitivity of $D(n)$ to the presence of the notch is shown by the coincidence of the solid and open symbols. Further, an empirical power-law of the form $D(n) = An^b$ describes the tensile data, and when extrapolated to $n > 8$ also describes the notched data on those cycles *in which no crack extension was observed*. Results similar to Figs 4(b) and 5(b) were obtained for the other six specimens.

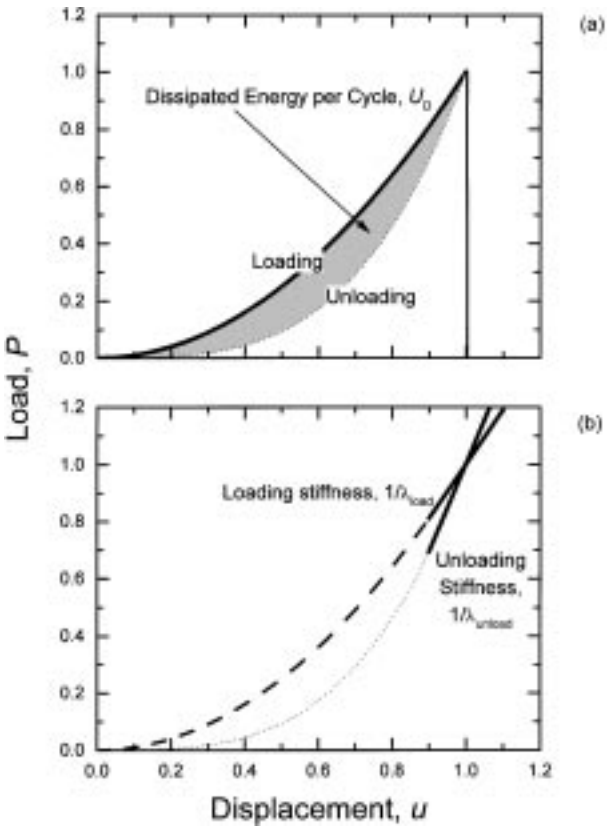

Figure 3 (a) Schematic diagram illustrating the total $U_T(n)$ and dissipated $U_D(n)$ energy for a single load–unload cycle; (b) Schematic diagram illustrating the method used to estimate loading and unloading compliance, ($\lambda = du/dP = 1/\text{stiffness}$).

3.3. Specimen compliance

Compliance values ($\lambda = du/dP$) were calculated by approximating a linear tangent to the top 15% of displacement on each loading and unloading curve (Fig. 3b). (If the unloading portion of the *P–u* curve on a cycle was initially vertical, those points were not included in the unloading compliance calculation, as a crack was continuing to propagate during initial unloading.)

Due to the quadratic nature of the load-displacement behavior of the tissue, it was discovered that the product of the compliance × displacement, λu, remained constant in the absence of cracking:

$$P = Bu^2$$
$$\lambda = du/dP = 1/2Bu$$
$$\lambda u = 1/2B = \text{constant}$$

where B is an empirical material-dependent coefficient and u is taken here as the peak displacement for that cycle. As the peak displacement level was changing every 4 cycles, this finding assisted in viewing of the compliance data and the detection of cracking.

Figs 4(c) and 5(c) show the measured loading and unloading compliance-displacement product λu as a function of cycle number n. As with the dissipated energy ratio $D(n)$, the compliance-displacement product λu for both loading and unloading showed little variation with n until crack extension occurred during the cycle ($n = 13$) at which point the λu products exhibited significant increases. Further changes in D and λu approximately paralleled each other for the remaining cycles – especially in Fig. 5. Similar variations in compliance associated *only* with observed crack extension were found for the other 6 specimens.

The finding that the increases in dissipated energy ratio and compliance were *only* observed on displacement cycles in which crack extension was also observed suggests two clear objective criteria for detection of fracture in neocartilage: (1) an increase in $D(n)$ above the level extrapolated for notched or unnotched specimens or (2) an associated increase in $\lambda_{load}(n)$ or $\lambda_{unload}(n)$ above the level extrapolated for notched specimens.

3.4. Fracture resistance analysis

The observation that the fractional dissipated energy $D(n)$ followed a predictable trend, and was the same for

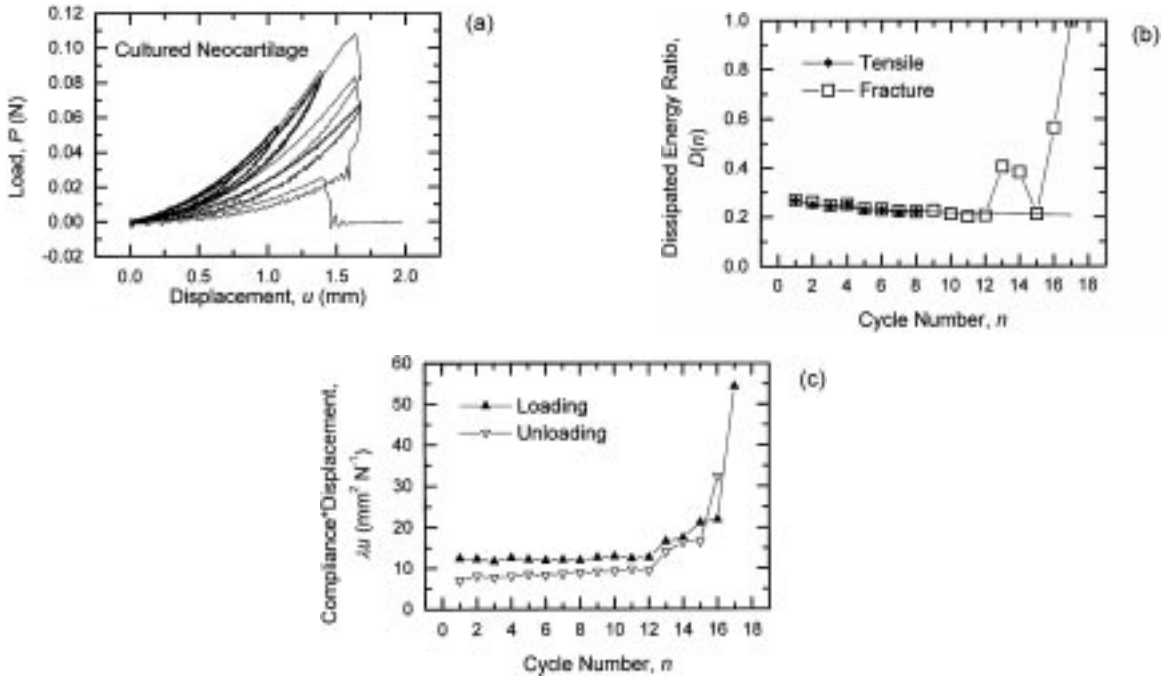

Figure 4 Plots showing behavior of cultured neocartilage during a notched fracture test: (a) load-displacement behavior, (b) dissipated energy as a function of cycle number, and (c) loading and unloading compliance as a function of cycle number. For this specimen initial crack extension was observed on cycle 13 and a crack arrest on cycle 15.

the same cycle number n in the (unnotched) tensile and (notched) fracture tests, has a deep implication. Although notching the specimen increased the stress in the remaining section – particularly near the notch root – the resulting invariance of $D(n)$ suggests that no additional mechanisms of viscoelastic deformation and loss were introduced, and that (at least over the range of stresses and strain rates used here) $D(n)$ is a material property. Viscoelastic and fracture contributions to $D(n)$ can therefore be treated as additive (in much the same way that delocalized dislocation shielding in semiconductors [11], transformation toughening in zirconia [12], and ligamentary wake bridging in ceramics [13] and composites [14] is separated from localized crack-tip bond rupture). This additivity provides a method for estimating the fracture resistance of neocartilage.

A base fractional dissipation can be defined as $D_0(n)$, in which the 0 subscript indicates the absence of a moving crack, independent of the presence or absence of notching in the specimen. Thus $D_0(n) = D(n)$ in the absence of cracking, and $D_0(n) < D(n)$ when a crack is actively propagating and actively dissipating energy. The amount of energy dissipated due to fracture U_F can be calculated from the total measured dissipated energy U_D

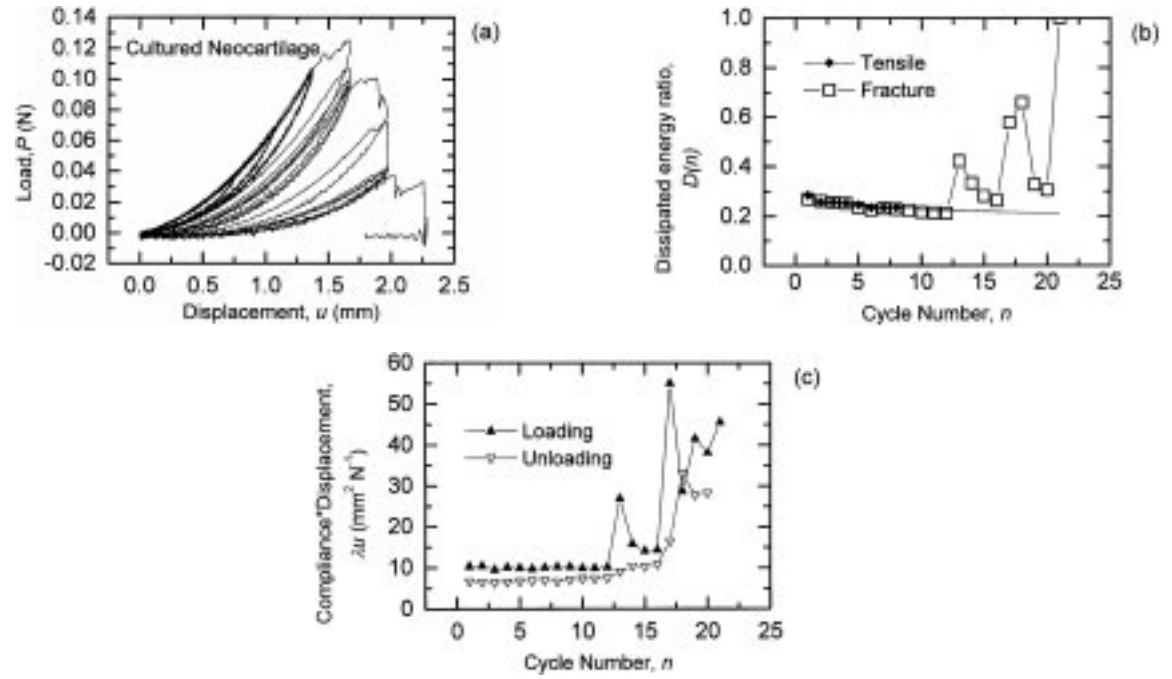

Figure 5 Plots showing behavior of cultured neocartilage during a notched fracture test: (a) load-displacement behavior, (b) dissipated energy as a function of cycle number, and (c) loading and unloading compliance as a function of cycle number. For this specimen initial crack extension was observed on cycle 13 and crack arrest events on cycles 16 and 20.

by subtracting off the ''predictable'' energy dissipation due to viscoelasticity:

$$U_F(n) = U_D(n) - U_T(n)D_0(n) \quad (2)$$

By definition, $U_D(n) = U_T(n)D(n)$ (Equation (1)) and therefore

$$U_F(n) = U_T(n)[D(n) - D_O(n)] \quad (3)$$

The fracture energy per cycle $U_F(n)$ can then be used in calculations of the fracture resistance $R(n)$, where

$$R(n) = U_F(n)/[t\Delta c(n)] \quad (4)$$

and $\Delta c(n)$ is the incremental increase in crack length during cycle n. The total crack length after each cycle is then $c(n) = \sum \Delta c(n)$.

Using Equations (3) and (4), the R-curves, $R(n)$ versus $c(n)$, were constructed for the samples in Figs 4 and 5 and are shown as the solid symbols in Fig. 6. The initial crack extensions for these specimens were 0.5 and 1 mm, respectively. Also shown in as open symbols is the fracture resistance variation of an additional specimen that exhibited smaller initial crack extensions. Interestingly, in this case, the fracture resistance exhibited an increase at short cumulative crack length and a tendency to a plateau at longer crack lengths.

4. Discussion

The dissipated energy in a single loading cycle was near 20–25% of total energy for the cultured neocartilage. This compares reasonably values for other soft biological tissues, such as 7% for plantaris tendon and 30% for human heel pad [1]. The dissipated energy ratio $D_0(n)$ may be directly related to the tissue constituents and microstructure; tendon is mostly collagenous with little proteoglycan, while heel pad is primarily lipid with very little collagen. However, the dissipated energy ratio appears not scale with differences in tissue stiffness, as the reported tensile modulus for tendon (1500 MPa) is several orders of magnitude greater than that for heel pad (5 MPa) [1] and neocartilage (1.3 MPa) [10].

On fracture, the dissipated energy in the neocartilage approximately (only) doubles to 40–60%. Admittedly, this increase is geometry dependent, but points to the need for understanding of viscoelastic processes before (a) interpretation of fracture mechanics tests or (b) development of fracture models. In addition, further investigation of the relationship between dissipated energy and tissue composition is also called for in future studies in order to understand the prefailure behavior of the matrix.

Nevertheless, an implication of Fig. 6 is that the fracture resistance, or toughness, of neocartilage is determined by a cumulative process that exhibits a transient increase at short crack lengths and a steady-state plateau for long cracks, in much the same way as many non-biological systems [11–14]. Given the fibrillar composite microstructure of cartilage and the relative insensitivity of $D(n)$ to notching, it is tempting in this case to associate the R-curve behavior with the formation of a bridging crack-wake zone (controlled by crack-opening displacement) [13, 14] rather than with the formation of a shielding crack frontal zone (controlled by crack-tip stress field) [11, 12]. An interpretation of the data for the samples from Figs 4 and 5 is that the initial large crack extension precluded observation of the transient fracture resistance and that the data reflect a plateau state. A previous investigator calculated tear toughness in cartilage to be 0.14–1.2 kJ m^{-2} [9]. This range of values agrees surprisingly well with the data in this experiment (plateau values of 0.2–0.45 kJ m^{-2}), considering the compositional and microstructural differences between native and cultured cartilage.

Clearly, the techniques described here for both identification of crack extension and estimation of fracture resistance offer great promise for biological materials in general. In particular, the techniques are well suited for comparisons of cartilage (and neocartilage) in natural, altered, and diseased states and should provide insight into the effects of microstructure on resistance to both deformation and fracture. Additionally, the lack of assumption regarding the nature of the strains (linear versus nonlinear, small versus large) during fracture suggests the techniques could be well applied to other membranous biological tissues that exhibit extremely large strains to failure.

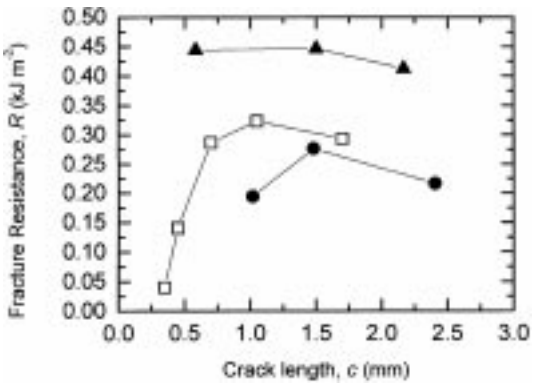

Figure 6 Plots of the fracture resistance R as a function of the cumulative crack length $c(n)$ (R-curves) for cultured neocartilage. Solid symbols indicate data for samples in Figs 4 and 5. Open symbols indicate data from an additional sample in which the initial crack increments were small, allowing the increase in fracture resistance with crack length to be observed.

Acknowledgments

The authors wish to acknowledge helpful discussions with Prof. Jack Lewis. Partial support for this work was provided by the NSF Graduate Fellowships Program (M. O.-T.) and the Artificial Tissues Program within the NSF Materials Research, Science and Engineering Center at the University of Minnesota.

References

1. R. F. KER, *J. Exper. Biol.* **202** (1999) 3315.
2. V. ROTH and V. C. MOW, *J. Bone Joint Surg. [Am.]* **62A** (1980) 1102.
3. G. E. KEMPSON, H. MUIR, C. POLLARD, M. TUKE, *Biochim. Biophys. Acta* **297** (1973) 456.
4. G. E. KEMPSON, *Biochim. Biophys. Acta* **1075** (1991) 223.

5. L. A. SETTON, V. C. MOW, F. J. MULLER, J. C. PITA, D. S. HOWELL, *J. Orthop. Res.* **12** (1994) 451.
6. H. M. FROST, *Anat. Rec.* **255** (1999) 162.
7. J. A. BUCKWALTER and H. J. MANKIN, *J. Bone Joint Surg. [Am.]* **79A** (1997) 612.
8. D. T. FELSON and Y. ZHANG, *Arthritis Rheum.* **41** (1998) 1343.
9. M. V. CHIN-PURCELL and J. L. LEWIS, *ASME J. Biomech. Eng.* **118** (1996) 545.
10. M. M. FEDEWA, T. R. OEGEMA Jr., M. H. SCHWARTZ, A. MACLEOD, J. L. LEWIS, *J. Orthop. Res.* **16** (1998) 227.
11. P. B. HIRSCH, S. G. ROBERTS and J. SAMUELS, *Proc. R. Soc. Lond.* A **421** (1989) 25.
12. R. M. MCMEEKING and A. G. EVANS, *J. Am. Ceram. Soc.* **65** (1982) 242.
13. R. F. COOK, *Acta Metall. Mater.* **38** (1990) 1083.
14. D. B. MARSHALL, B. N. COX, A. G. EVANS, *Acta Metall.* **33** (1985) 2013.

Received 13 March
and accepted 3 August 2000